

# The structure of $\gamma$ -polypivalolactone: a combined analysis of single-crystal electron diffraction data and powder X-ray diffraction profiles with the Rietveld method

S. V. Meille and S. Brückner

*Dipartimento di Chimica, Politecnico di Milano, Piazza Leonardo da Vinci 32, I-20133 Milan, Italy*

and J. B. Lando

*Department of Macromolecular Science, Case Western Reserve University, Cleveland, Ohio 44201, USA*

*(Received 8 August 1988; accepted 6 October 1988)*

The crystal structure of the  $\gamma$ -phase of polypivalolactone ( $\gamma$ -PPVL) has been determined from electron diffraction data and tested with the Rietveld method against X-ray powder diffraction profiles. The electron diffraction study is based on single-crystal patterns obtained from melt-crystallized solution-cast thin films, while the Rietveld analysis was performed on data from melt-crystallized samples containing comparable amounts of  $\alpha$ - and  $\gamma$ -phase PPVL. The crystal class is orthorhombic (space group  $P2_12_12_1$ ), and two molecules with the same chirality and opposite directions pass through the unit cell having lattice dimensions  $a = 8.23$ ,  $b = 11.28$ ,  $c(\text{chain repeat}) = 6.02$  Å. Both  $hk0$  and tilted-specimen electron diffraction data were used in the refinement, carried out in the kinematic approximation. The analysis based on these data and on powder profiles coherently indicates that the refined structural model has a main-chain conformation intermediate between the one found in the  $\alpha$ -phase and the minimum-energy conformation, while differing significantly from both.

**(Keywords:  $\gamma$ -polypivalolactone; electron diffraction; Rietveld method; X-ray diffraction)**

## INTRODUCTION

Crystal structure analysis by electron diffraction has been successfully applied to polymers because chain-folded crystals are of minimal thickness and generally consist of light atoms. These factors limit the dynamic scattering effects and in some cases<sup>1,2</sup> the kinematic treatment has been shown to be adequate. In other instances, however, when strong space-group-forbidden reflections are apparent or crystal deformation important, or the unit-cell axis parallel to the beam is long, quantitative kinematic treatment may lead to models of low accuracy<sup>3,4</sup>. Some of the limitations of the crystal structures of polymers obtained from electron diffraction data analysis may also relate to the use of reflections from a single reciprocal lattice net.

A possible procedure to evaluate the validity of the structural models obtained by treating electron diffraction data kinematically is to compute the perturbation of the data due to  $n$ -beam diffraction<sup>1-3,5</sup>. In the present study we have chosen a different approach, i.e. to test the various models obtained from refinement with electron diffraction data against a completely independent powder profile data set. We have recently shown<sup>6,7</sup> that powder profiles can in favourable instances be highly discriminatory towards unsatisfactory structural models while allowing for a comparatively straightforward treatment of experimental data. We believe consistency of a

particular model with two independent data sets to be a comparatively stringent validating procedure.

In the present paper the above approach is applied to the crystal structure of  $\gamma$ -polypivalolactone ( $\gamma$ -PPVL). This phase<sup>8,9</sup> always coexists with variable amounts of the higher-melting  $\alpha$ -modification. Depending upon crystallization conditions and on heat transfer efficiency, i.e. also on sample size, the relative proportions may vary from pure  $\alpha$ -phase (samples crystallized from the melt above 140°C, solution-crystallized material), to a predominant  $\gamma$ -content in very thin films crystallized from the melt at approximately 100°C. Attempts to crystallize the  $\gamma$ -phase crystals from solution or to obtain oriented samples adequate for fibre diffraction studies have so far been unsuccessful.

Preliminary data on the  $\gamma$ -phase of polypivalolactone have been reported in a previous paper<sup>9</sup>, while a solid-state n.m.r. investigation<sup>10</sup> of samples containing  $\alpha$ - and  $\gamma$ -PPVL has recently been published.

## EXPERIMENTAL

### *Electron diffraction*

Polypivalolactone supplied by the Tennessee Eastman Company was used in this study.

Samples for electron microscopy and diffraction were prepared with procedures already described in ref. 8.

Micrographs and diffraction patterns were recorded with a JEOL 100B electron microscope. Diffraction patterns were obtained operating in microbeam mode (approximate diameter 1200 Å). Kodak Electron Image film was used and integrated intensities were determined from radial scans with a Joyce-Loebel MKIII densitometer in the linear response range of the film. Data from different films or zones were scaled with common reflections. Following ref. 7 no Lorentz-polarization correction was applied to the data. Kinematic scattering was assumed in the data reduction while throughout the refinement the computer program LALS<sup>11</sup> was used with atomic scattering factors for electrons derived from scattering factors for X-rays<sup>12</sup>, making use of Mott's formula<sup>12</sup>.

#### X-ray diffraction

Samples suitable for X-ray diffraction were prepared following methods described elsewhere<sup>8,9</sup>.  $\gamma$ -Phase-rich samples for diffraction photographs were selected by inspecting films by optical microscopy to ensure that areas of predominantly  $\gamma$ -spherulites were exposed to the beam. Because of the larger amounts required (200 mg), this procedure could not be adopted for samples to be used in powder diffractometry, the relative  $\gamma$ -phase content being thus much lower. Diffraction photographs were recorded in a flat-film camera while diffraction profiles were recorded on a Siemens D-500 diffractometer. The most important data recording parameters are reported in Table 1.

### STRUCTURE ANALYSIS

#### Unit-cell and space-group determination

In a typical electron microscopy specimen two distinct diffraction patterns corresponding to areas with readily distinguishable morphologies<sup>9</sup> could be observed. One of the two diffraction patterns (Figure 1) indexes as the zero layer of the  $\alpha$ -phase of PPVL, while the  $d$ -spacings of the most intense reflections of the second (Figure 2) are in very good agreement with the X-ray data reported for the unoriented  $\gamma$ -form<sup>8</sup> (Table 2). Assuming this second pattern to be the  $hk0$  zone of the  $\gamma$ -phase, we were able to index also some diffraction photographs (Figures 3 and 4) obtained by tilting the specimen, with a  $c$  axis close to 6 Å, in a metrically orthorhombic unit cell. Least-squares refinement from X-ray data yielded the following lattice parameters:  $a = 8.23$ ,  $b = 11.28$ ,  $c$  (chain repeat) = 6.02 Å, the values obtained from electron diffraction data being  $\sim 0.01$ – $0.02$  Å larger. All the reflections  $h00$  and  $0k0$  respectively with  $h$  and  $k$  odd are unobserved except for the 100, the 010 and the 030 reflections, which are only apparent in  $hk0$  electron

Table 1 Experimental conditions of X-ray powder data recording

Instrument	Siemens D-500 goniometer equipped with step-scan attachment, proportional counter and Soller slits. Controlled with a Hewlett-Packard computer
Radiation (power)	Cu K $\alpha$ , Ni-filtered (40 kV, 30 mA)
Divergence aperture (deg)	0.3
Receiving aperture (deg)	0.05
Step width (deg)	0.05 ( $2\theta$ )
Count time, per step (s)	40
$2\theta$ range (deg)	9–60

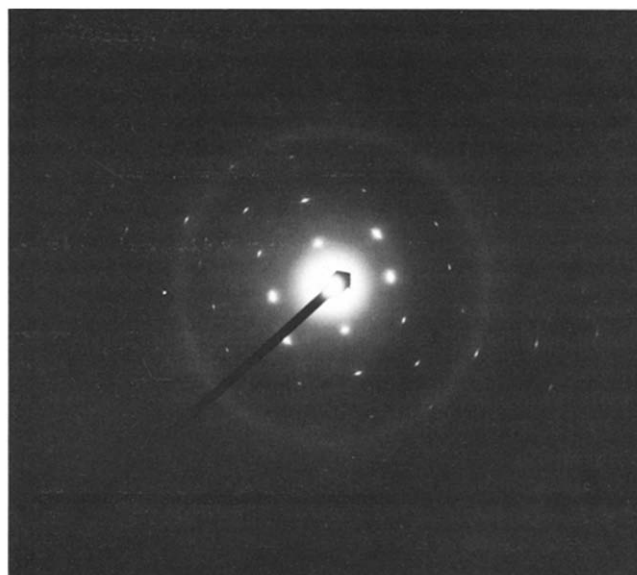


Figure 1 Electron diffraction pattern of the  $hk0$  reciprocal lattice plane of  $\alpha$ -PPVL

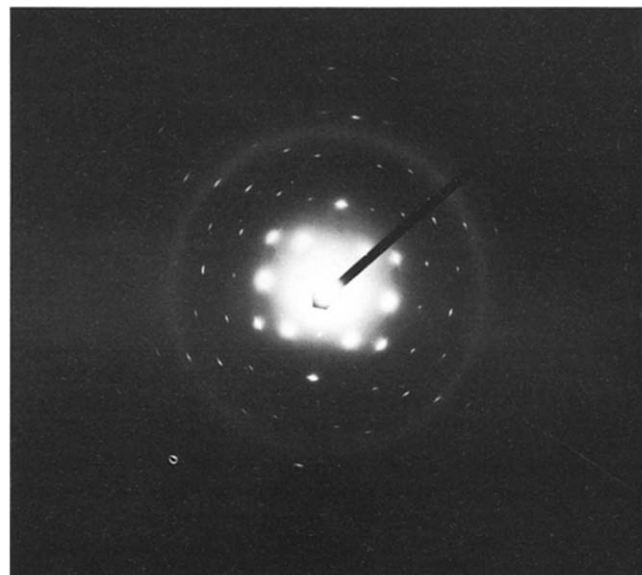


Figure 2 Electron diffraction pattern of the  $hk0$  reciprocal lattice plane of  $\gamma$ -PPVL

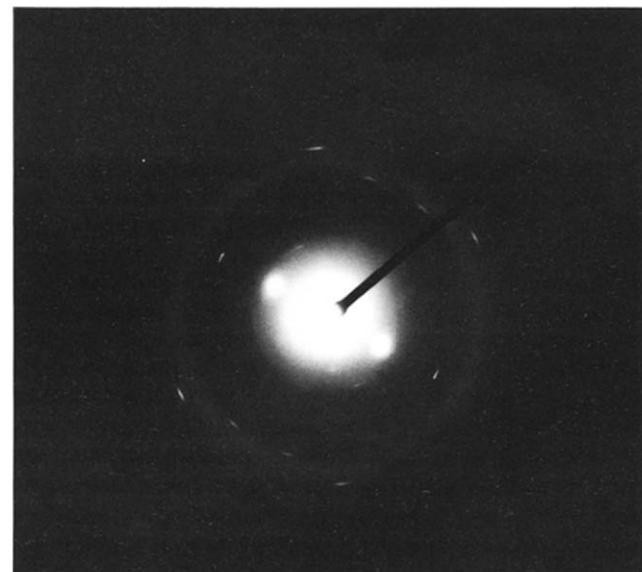
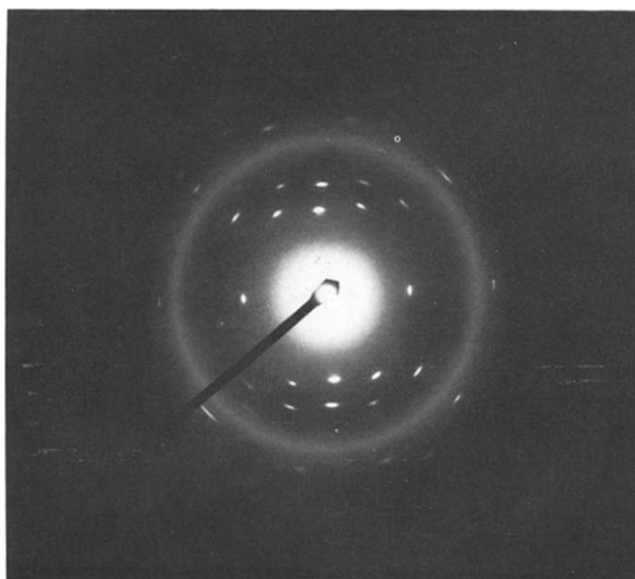


Figure 3 Tilted-specimen electron diffraction pattern of  $\gamma$ -PPVL. The  $3hkh$  reciprocal lattice plane and the  $2hkh$  planes can be recognized

**Table 2** A comparison of  $\gamma$ -phase PPVL  $d$ -spacings ( $\text{\AA}$ ) from X-ray diffraction photographs and electron diffraction patterns with the calculated values

X1 <sup>a</sup>	X2 <sup>b</sup>	E.d.	Calc.	$hkl$
6.67	6.66	6.68	6.65	110
5.61	5.64	5.63	5.64	020
	5.28		5.31	011
4.94	4.88		4.86	101
		4.67	4.65	120
4.48	4.46		4.46	111
4.04	4.13	4.15	4.12	021
		4.12	4.12	200
3.99				
	3.69	3.70	3.68	121
		3.44	3.42	130
	3.38	3.40	3.40	201
		3.32	3.32	220
3.16	3.19	3.19	3.19	031
			3.01	002
2.98	2.98	2.95	2.97	131
	2.89	2.92	2.91	221
			2.91	012
		2.82	2.82	040
		2.79	2.78	230
	2.72		2.74	112
	2.51	2.52	2.52	231
		2.50	2.50	301
		2.47	2.47	320

<sup>a</sup> Original values reported in ref. 8<sup>b</sup> Our data, sample annealed for 10h at 170°C**Figure 4** Tilted-specimen electron diffraction pattern of  $\gamma$ -PPVL. The  $h2k$ , the  $h3k$  and the  $h5k$  reciprocal lattice planes are shown

diffraction patterns. In tilted-crystal patterns and in X-ray diffraction photographs (Figure 5) these three reflections are absent, and we conclude that they arise from double diffraction effects involving  $hk0$  reflections. The  $00l$  class is the only one for which no electron diffraction data are available while X-ray data suggest the  $00l$  reflection to be unobserved. Furthermore the identity of the fibre repeat in the  $\alpha$ - and  $\gamma$ -phases supports the hypothesis that in the  $\gamma$ -modification the chain conformation should retain the  $2_1$  symmetry found in the  $\alpha$ -phase, implying  $00l$  with  $l$  odd extinction. Systematic absences are thus consistent with space group  $P2_12_12_1$  and this hypothesis was verified in the structure refinement.

The calculated density of the  $\gamma$ -phases, with four monomeric units in the unit cell, is  $1.190 \text{ g cm}^{-3}$ , to be compared with a calculated value of  $1.234 \text{ g cm}^{-3}$  for the  $\alpha$ -modification and an experimental density of  $1.21 \text{ g cm}^{-3}$  for samples containing comparable amounts of the two phases.

#### Electron diffraction

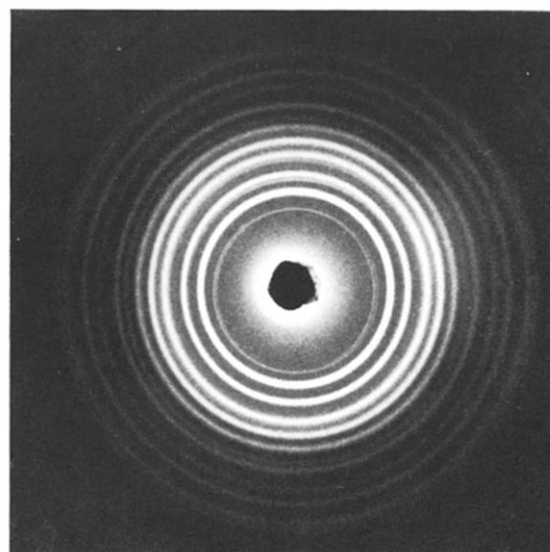
Refinement was carried out against 45  $hk0$  and 27 upper-layer reflections, all with  $d > 1.25 \text{ \AA}$ . The space-group-forbidden, weak 100, 010 and 030 reflections, appearing only in untilted electron diffraction patterns, were treated as unobserved.

The initial models in the structural analysis were those proposed for PPVL with the appropriate helical symmetry and repeat distance in previous work<sup>7,13,14</sup>. The more thoroughly refined structure obtained from X-ray analysis of the  $\alpha$ -phase<sup>7</sup> was taken as one starting model (model I), while as the second (model II) we chose the structure proposed by Cornibert *et al.*<sup>14</sup> on the basis of an energy-minimization calculation for the isolated helix. The first step in the analysis was a rigid-body refinement of model I and model II. Coincidence of the helix axis with the crystallographic  $2_1$  axis parallel to  $c$  reduced the adjustable parameters to the rotation and the translation of the coupled chains about their axis. A common isotropic temperature factor was also refined while adjustments of the main-chain torsion angles of less than one degree were tolerated. The resulting agreement factors

$$R = \frac{\sum [|F_i(\text{obs})| - |F_i(\text{calc})|]^2}{\sum [F_i(\text{obs})]^2}$$

were 0.21 for model I and 0.29 for model II with temperature factors  $B$  of 4.1 and  $4.3 \text{ \AA}^2$  respectively for only the zero-layer reflections. Including all data,  $R$  values of 0.17 for model I and 0.22 for model II with  $B$  values of  $5.5 \text{ \AA}^2$  for both models were obtained (see Table 3).

These preliminary structural models were the starting points of subsequent refinements in which also all torsion angles were varied, and minor bond-angle adjustments were allowed while keeping the refined structure stereo-

**Figure 5** X-ray diffraction pattern of  $\gamma$ -PPVL annealed for 10h at 170°C under vacuum. Low-intensity, eccentric rings are due to  $\alpha$ -phase impurities

**Table 3** A comparison of main-chain torsion angles (deg), and disagreement factors for the three models studied

	$\tau_1$	$\tau_2$	$\tau_3$	$\tau_4$	$R_{e.d.}^a$	$R_{Rietveld}$
Model I <sup>b</sup>	46	54	191	182	0.17	0.105
Model II <sup>c</sup>	60	34	180	208	0.22	0.112
Model III <sup>d</sup>	52	48	178	195	0.14	0.094

<sup>a</sup> All data,  $h00$  and  $0k0$  data from tilted-specimen patterns<sup>b</sup>  $\alpha$ -Phase, ref. 7<sup>c</sup> Minimum-energy conformation, ref. 14<sup>d</sup>  $\gamma$ -Phase, this work**Table 4** Final positional parameters of model III (isotropic thermal factor  $B=6.0 \text{ \AA}^2$ )

Atom	$x$	$y$	$z$
C1	0.1941	-0.1177	-0.3226
C2	0.0510	-0.0779	-0.1778
C3	0.1028	0.0329	-0.0492
C4	0.0032	-0.1789	-0.0183
C5	-0.0980	-0.0532	-0.3262
O1	0.2499	0.0186	0.0472
O2	0.0100	0.1175	-0.0250
H1-1	0.2927	-0.1494	-0.2170
H2-1	0.1550	-0.1888	-0.4330
H1-4	0.1023	-0.1950	0.0984
H2-4	-0.1061	-0.1539	0.0733
H3-4	-0.0205	-0.2593	-0.1134
H1-5	-0.0797	0.0296	-0.4163
H2-5	-0.1132	-0.1256	-0.4445
H3-5	-0.2066	-0.0461	-0.2230

chemically acceptable. Also in this second step refinements were carried out against all available data and for the sake of comparison, utilizing only the  $hk0$  or the tilted data sets.

With all data sets the final structural models depend only marginally upon the starting points. In fact the differences in the refined parameters are comparable with the estimated standard deviations. The minimum determined from the  $hk0$  refinement appears, however, to be somewhat broader than the ones obtained from all data or from tilted-specimen data. The final disagreement factors for the final structure (model III) were 0.14 with a temperature factor of  $6.0 \text{ \AA}^2$ , while for the essentially identical structural model obtained for  $hk0$  projection data and tilted-specimen data, respectively, final  $R$  factors of 0.16 and 0.08 with  $B$  factors of 3.9 and  $8.2 \text{ \AA}^2$  were obtained.

In Table 3 the essential structural features for the most relevant of the examined structural models are reported together with the corresponding disagreement factors, while in Tables 4, 5 and 6 respectively the final positional parameters of model III, the corresponding refined internal coordinates, with estimated standard deviations, and a list of observed and calculated structure factors are listed. The numbering scheme of the PPVL chain is shown in Figure 6 while in Figure 7 a packing diagram of the  $\gamma$  unit cell is shown.

#### Rietveld analysis

The presence in the sample utilized for the powder data collection of both  $\alpha$  and  $\gamma$  crystalline phases in approximately equivalent amounts suggests a very prudent use of the Rietveld approach in the investigation of the  $\gamma$ -PPVL crystal structure. We decided to adopt the

**Table 5** Chain geometry of model III

Bond lengths (Å)	
C1-C2	1.53
C2-C3	1.53
C2-C4	1.54
C2-C5	1.54
O1-C1'	1.44
C3-O1	1.35
C3-O2	1.23
C-H	1.09
Bond angles (deg)	
C2-C1-O1'	109.1(1.2)
C1-C2-C3	108.3(1.4)
C1-C2-C4	109.5
C1-C2-C3	109.5
C2-C3-O1	111.7(1.4)
C2-C3-O2	121.4(2.5)
C3-O1-C1'	115.3(1.9)
Torsion angles (deg)	
C3-O1-C1'-C2'	194.5(2.5)
C1-C2-C3-O1	47.7(2.9)
C1-C2-C3-O2	-138.6(3.9)
C2-C3-O1-C1'	178.3(2.5)
O1-C1'-C2'-C3'	52.2(2.3)
O1-C1'-C2'-C4'	173.4(2.4)
O1-C1'-C2'-C5'	-69.5(2.6)

**Table 6** Observed<sup>a</sup> and calculated structure factors for model III

$h$	$k$	$l$	$F_{obs}$	$F_{calc}$	$h$	$k$	$l$	$F_{obs}$	$F_{calc}$
2	0	0	137	149	4	7	0	8 <sup>b</sup>	5
4	0	0	58	60	5	1	0	62	46
0	2	0	264	247	5	2	0	8 <sup>b</sup>	1
0	4	0	51	51	5	3	0	12	16
0	6	0	16	16	5	4	0	11	9
0	8	0	8 <sup>b</sup>	2	5	5	0	8 <sup>b</sup>	2
1	1	0	171	184	6	1	0	16	12
1	2	0	145	151	6	2	0	53	48
1	3	0	48	5	6	3	0	27	28
1	4	0	45	20	2	0	1	106	120
1	5	0	17	17	3	0	1	17	16
1	6	0	34	38	3	1	1	71	82
1	7	0	29	29	0	2	1	203	203
1	8	0	11	6	1	2	1	133	120
2	1	0	29	10	2	2	1	110	102
2	2	0	47	51	4	2	1	28	34
2	3	0	63	40	5	2	1	19	22
2	4	0	59	55	0	3	1	169	161
2	5	0	54	52	1	3	1	93	80
2	6	0	28	30	2	3	1	41	43
2	7	0	44	35	3	3	1	85	90
2	8	0	24	25	4	3	1	19	21
3	1	0	46	40	5	3	1	37	32
3	2	0	44	48	3	4	1	15	16
3	3	0	27	17	3	5	1	19	24
3	4	0	17	25	0	4	2	37	33
3	5	0	21	13	1	4	2	98	114
3	6	0	59	48	2	4	2	60	76
3	7	0	27	26	0	5	2	19	17
3	8	0	13	12	1	5	2	51	52
4	1	0	38	25	2	5	2	12 <sup>b</sup>	15
4	2	0	21	23	3	5	2	12 <sup>b</sup>	9
4	3	0	30	19	0	6	2	60	63
4	4	0	36	25	1	6	2	12 <sup>b</sup>	14
4	5	0	8 <sup>b</sup>	7	2	6	2	12 <sup>b</sup>	9
4	6	0	8 <sup>b</sup>	11	3	6	2	12 <sup>b</sup>	24

<sup>a</sup>  $h00$  and  $0k0$  observed values from tilted-specimen data<sup>b</sup> Unobserved, subthreshold value reported

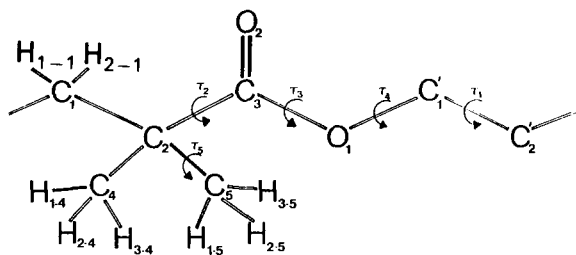


Figure 6 The PPVL chain: definition of the nomenclature used in the tables and in the text

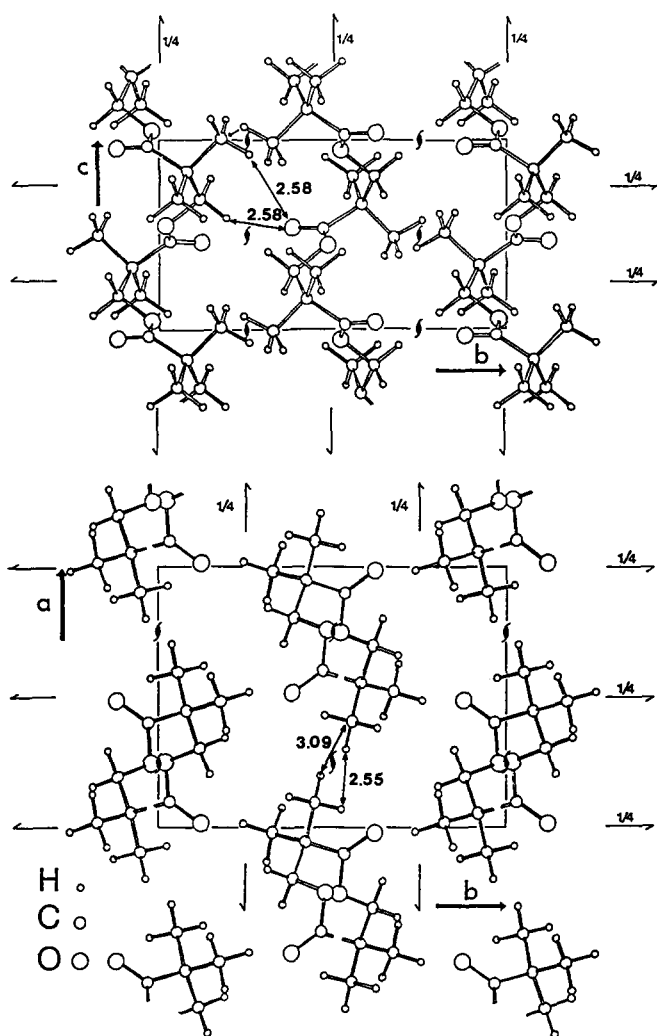


Figure 7 Packing diagram of  $\gamma$ -PPVL (model II); relevant inter-molecular distances (Å) are shown

observed powder X-ray diffraction profile (Figure 8) only as a discriminating test for the  $\gamma$ -phase structural models proposed on the basis of electron diffraction data. No attempt was made to refine structural parameters according to the usual<sup>15</sup> least-squares procedure.

Since the  $\alpha$ -PPVL crystal structure has already been determined<sup>7,13</sup>, its contribution to the observed profile was evaluated once and for all in a preliminary calculation and stored in the memory of the computer. The least-squares routine of Immirzi<sup>15</sup> was then modified by one of the authors in order to take into consideration this extra contribution and to allow for the refinement of the corresponding scale factor. The overall calculated profile is therefore the superposition of the properly scaled

profiles of the  $\alpha$ - and  $\gamma$ -phases. Non-structural parameters such as peak shapes, half-height widths, preferred orientation of the crystallites and zero correction on the experimental  $2\theta$  scale, as well as background contributions, were refined in the usual way<sup>15</sup>.

The three structural models already tested against electron diffraction data were thus taken into consideration and their computed profiles compared with the observed powder diffraction diagram. The three disagreement factors, computed in the form

$$\left\{ \sum w_i [y_i(\text{obs}) - y_i(\text{calc})]^2 / \sum [w_i y_i(\text{obs})]^2 \right\}^{1/2}$$

are 10.5%, 11.1% and 9.4% for models I, II and III respectively. The discriminating power of the observed profile appears to be low due to the co-presence of the  $\alpha$ -phase; however, the differences are significant and they confirm the results obtained by the analysis of electron diffraction data with a completely independent procedure. In Figure 8 we show the comparison between the observed profile (curve A) and the profile calculated with model III (curve B), while also considering the pre-evaluated contribution of the  $\alpha$ -phase; curve C is the difference profile while the dotted curve is the background contribution. From the refined scale factors we get an estimate of the relative amounts of  $\alpha$ - and  $\gamma$ -phases. They are 57% and 43% respectively, a rather unfavourable ratio that is substantially due to the need to use samples of approximately 200 mg. A much better ratio could have been achieved by working with microsamples and photographically recorded powder diffraction diagrams. In Table 7 we report the non-structural parameters refined for model III and those adopted for the evaluation of the  $\alpha$ -phase contribution.

A last remark concerns the improvements to the routine of Immirzi for the treatment of peak asymmetry, a feature that usually affects peaks at low diffraction angle and progressively vanishes at increasing  $2\theta$  values<sup>16</sup>. According to the new procedure each peak is built by juxtaposing two half-peaks with different half-height widths  $H'_k$  and  $H''_k$ , while keeping the overall integrated intensity constant. The  $2\theta$  dependence of this effect was taken into account by assuming the difference  $H'_k - H''_k$  to vary with  $2\theta$  as  $A/(2\theta)^2$  where  $A$  is an adjustable parameter. This is of course a completely empirical approach, the validity of which is only supported by

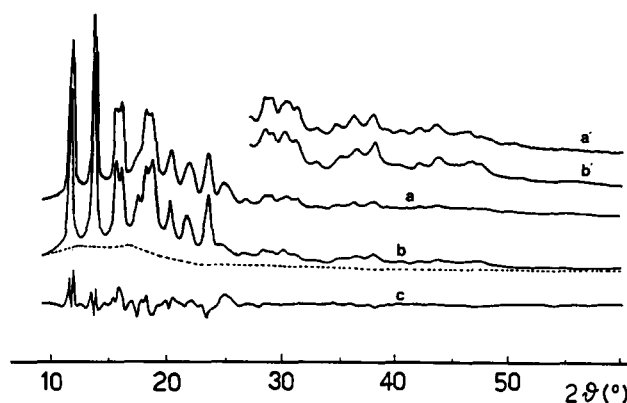


Figure 8 The experimental powder profile (curve a) of a PPVL sample containing similar amounts of  $\alpha$ - and  $\gamma$ -phase. Curve b and curve c are the calculated and the difference profiles respectively while the dotted curve is the calculated background contribution

**Table 7** Rietveld non-structural parameters adopted in the computation of the overall ( $\alpha$ - plus  $\gamma$ -phases) profile

	$\gamma$ -phase (model III)	$\alpha$ -phase
Scale factor	1.00	1.34
Preferred orientation parameter <sup>a</sup>	0.06(2)	0.20(5)
Peak shape parameters <sup>b</sup>		
<i>U</i>	15(3)	6.5(8)
<i>V</i>	1.0(1)	1.1(2)
<i>W</i>	-0.16(1)	-0.07(3)
<i>m</i>	1	1
Zero correction $2\theta$ (deg)	-0.17(1)	-0.17(1)

Background intensities (*k* count) at nodes of the segmented line

$2\theta$ (deg)	<i>k</i> count
9	0.98(4)
12	1.61(4)
14.5	1.29(5)
16.5	1.46(6)
19.5	0.68(5)
22.5	0.22(6)
26	0.40(3)
30	0.30(3)
36	0.25(2)
39	0.15(2)
42	0.25(2)
46	0.13(2)
60	0.14(2)

<sup>a</sup> Preferred orientation factor is  $PO = \exp(-G\alpha_k)$ , where  $\alpha_k$  is the angle between the scattering vector of the *k*th reflection and the scattering vector of a fixed (preferred) orientation, in this case the [100] reflection for the  $\alpha$ -phase and the [110] reflection for the  $\gamma$ -phase

<sup>b</sup> According to the relation  $H_k^2 = U \tan^2 \theta_k + V \tan \theta_k + W$ ; *m* is the exponent in the Pearson VII profile function

$$f(z) = (C/H_k)[1 + 4(2^{1/m} - 1)z^2]^{-m},$$

$$\text{with } z = (2\theta_i - 2\theta_k)/H_k$$

significant improvement in the reproduction of observed data.

## DISCUSSION

The values of the disagreement factors with reasonable temperature factors (see Table 3) obtained in the rigid-body refinement of model I supports the initial assumption, corroborated by recent n.m.r. results<sup>10</sup>, that the overall conformation of PPVL in the  $\alpha$ - and  $\gamma$ -phases should be similar. Also the fit of both the electron diffraction and X-ray data sets with the proposed minimum-energy isolated chain<sup>14</sup> (model II), although less satisfactory than for model I, is remarkable. It is therefore not surprising that the final refined structure of  $\gamma$ -PPVL (model III) should lie within the range of the conformational hyperspace roughly delimited by the  $\alpha$ -modification structure (model I) and the minimum-energy conformation (model II). Also the packing of model III appears to be qualitatively sound (see Figure 7) as no unlikely intermolecular interactions are found, and we can safely state that the refined structural model is stereochemically reasonable and intrinsically acceptable. It seems of interest in this context to note that, consistent with the chiral nature of the  $\gamma$ -phase space group (P2<sub>1</sub>2<sub>1</sub>2<sub>1</sub>), PPVL in block copolymers with chiral poly( $\alpha$ -methyl- $\alpha$ -propyl)- $\beta$ -propiolactone<sup>17</sup> shows a marked tendency to crystallize in the  $\gamma$ -phase rather than in the achiral  $\alpha$ -modification.

In order properly to evaluate the degree of confidence to be given to the fully refined  $\gamma$ -phase conformation (model III), the following considerations appear relevant: (i) Electron diffraction (on both zero-layer and tilted-specimen data), and Rietveld analysis disagreement factors are completely coherent for all the examined models; the worst result is always obtained with model II, while the analysis with all data sets clearly favours model III over model I. (ii) The refined temperature factors *B* obtained with all three models are 4 Å<sup>2</sup> for *hk0* projection data and 8 Å<sup>2</sup> for tilted data, while using the complete data set an average value of 6 Å<sup>2</sup> is calculated. These figures compare well with the *B* value of 6.2 Å<sup>2</sup> determined from fibre data for  $\alpha$ -PPVL. They suggest<sup>2</sup> that in the present case multiple scattering effects are negligible in tilted data and somewhat more important (consistent with the appearance of space-group-forbidden reflections) in *hk0* reflections from untilted specimens. Accordingly all the examined models show a considerably better agreement with the tilted data than with the *hk0* projection.

The above analysis allows us to conclude that in the case of the present work non-kinematic scattering is modest and its impact on the final refined model is low. The determined differences between the  $\gamma$ - and  $\alpha$ -PPVL conformations, though small, are therefore very likely to be significant, e.g. for  $\tau_3$  and  $\tau_4$  (see Table 3), which differ in the two phases by  $\sim 15^\circ$ , while the estimated standard deviations are of the order of  $3^\circ$  (Table 5). Certainly a complete Rietveld refinement of  $\gamma$ -PPVL to produce an independent structural model would have been an even more stringent verification, but it was impossible with the available diffractometer data due to the co-presence of  $\alpha$ - and  $\gamma$ -phases in nearly equal amounts. In this respect we note that the possibility of refining the overall contributions of two different crystalline phases to the observed profile represents a novel and accurate way of determining their relative amounts. In fact the two scale factors are substantially independent of effects like preferred orientation, which may affect individual peak intensities and distort evaluations based on such data.

We remark finally that, given a 20°C difference in melting points<sup>8</sup>, the stability of the  $\alpha$ - and  $\gamma$ -phases should be only slightly different. It appears reasonable that the  $\gamma$ -modification, with a markedly lower density than the  $\alpha$ -phase, should be characterized by a chain conformation closer to the minimum-energy structure (model II) for the isolated molecule. Thus in  $\gamma$ -PPVL the less favourable intermolecular interactions could possibly be compensated by a chain conformation more stable than in the  $\alpha$ -polymorph. Detailed packing energy calculations, which also involve the above issue, will be presented in a forthcoming paper.

## ACKNOWLEDGEMENTS

A portion of the present work was carried out at Case Western Reserve University while the remainder was done at Politecnico di Milano. Encouraging discussions with Professor P. H. Geil are acknowledged.

## REFERENCES

- 1 Claffey, W., Gardner, K. H., Blackwell, J., Lando, J. B. and Geil, P. H. *Phil. Mag.* 1974, **30**, 1223

**Structure of  $\gamma$ -polypivalolactone: S. V. Meille et al.**

- 2 Moss, B. and Dorset, D. L. *J. Polym. Sci., Polym. Phys. Edn.* 1982, **20**, 1789
- 3 Moss, B. and Dorset, D. L. *Polymer* 1983, **24**, 291
- 4 Dorset, D. L. *Acta Crystallogr. (A)* 1976, **32**, 207
- 5 Dorset, D. L. *J. Electron Microsc. Techn.* 1985, **2**, 89
- 6 Bruckner, S., Meille, S. V., Malpezzi, L., Cesaro, A., Navarini, L. and Tombolini, R. *Macromolecules* 1988, **21**, 967
- 7 Bruckner, S., Meille, S. V. and Porzio, W. *Polymer* 1988, **29**, 1586
- 8 Prud'homme, R. E. and Marchessault, R. H. *Makromol. Chem.* 1974, **175**, 2705
- 9 Meille, S. V., Konishi, T. and Geil, P. H. *Polymer* 1984, **25**, 773
- 10 Veregin, R. P., Fyfe, C. A. and Marchessault, R. H. *Macromolecules* 1986, **19**, 2379
- 11 Campbell Smith, P. J. and Arnott, S. *Acta Crystallogr. (A)* 1978, **34**, 3
- 12 'International Tables for X-ray Crystallography', Kynoch Press, Birmingham, 1974, Vol. III
- 13 Perego, G., Melis, A. and Cesari, M. *Makromol. Chem.* 1972, **157**, 269
- 14 Cornibert, J., Hien, N. V., Brisse, F. and Marchessault, R. H. *Can. J. Chem.* 1974, **52**, 3742
- 15 Immirzi, A. *Acta Crystallogr. (B)* 1980, **36**, 2378
- 16 Klug, H. P. and Alexander, L. E. 'X-Ray Diffraction Procedures', Wiley, New York, 1974
- 17 Allegrezza, A. E., Lenz, R. W., Cornibert, J. and Marchessault, R. H. *J. Polym. Sci., Polym. Phys. Edn.* 1978, **16**, 2617